NANO LETTERS

pubs.acs.org/NanoLett

Composite Au Nanostructures for Fluorescence Studies in Visible Light

V. G. Kravets,[†] G. Zoriniants,[‡] C. P. Burrows,[‡] F. Schedin,[†] A. K. Geim,[†] W. L. Barnes,[‡] and A. N. Grigorenko*[,†]

[†]School of Physics and Astronomy, University of Manchester, Manchester, M13 9PL, U.K. and [‡]School of Physics, University of Exeter, Stocker Road, Exeter, EX4 4QL, U.K.

ABSTRACT We present results from composite plasmonic nanostructures designed to achieve the cascaded enhancement of electromagnetic fields at optical frequencies. Our structures comprise a small metallic nanodisc suspended above a larger disk. We probe the optical properties of these structures by coating them with a layer of a visible-light fluorophore and observing fluorescence signals with the help of scanning confocal microscopy. A 43 ± 5-fold increase in the far-field fluorescence signal has been observed for two-tier composite nanostructures, when compared to the signal obtained from individual nanodiscs. Our results offer the prospect of using such nanostructures for field concentration, optical manipulation of nanoobjects, chemical and biological sensing.

KEYWORDS Plasmonics, nanostructures, field enhancement, giant fluorescence

Strong enhancements of electromagnetic fields are essential in nonlinear optics[1,2] photochemistry and biophysics[3−5] and light-matter interactions.[6,7] Metallic nanoparticles allow one to achieve a high value of field enhancement through the excitation of localized surface plasmons.[1,2,8−18] Strong near-fields promise exciting applications in different areas of science and technology, for example, Raman or fluorescence studies with single molecule sensitivity.[16−18] The field strength can be increased even further in particle conglomerates, such as fractals,[9] particle dimers[10,11] and aggregates,[12] which can be effectively used for manipulation of nano-objects[13,14] and chemical and biological sensing.

There are two types of nanostructured materials that have been pursued recently for optical field enhancement. One involves regular, well-defined single nanostructures, for example, optical antennas.[1,10,11,15] Large field-enhancements have been demonstrated for nanoantennas by measuring nonlinear photon conversion from electrons inside the metal or dilute plasma outside.[1,10,11,15] It remains to be seen if such structures (mostly working in the infrared) could be successfully applied for practical Raman and fluorescence measurements in the visible; for recent progress see review.[16] The other structural type is based on more complex nanostructures, typically aggregates of nanoparticles formed by chemical synthesis. Such structures have been the focus of a number of reports on strongly enhanced Raman scattering[17] or fluorescence[18] where the enhancement is often attributed to some "hot" nanoparticles (or rough substrate). The sensitivities demonstrated in these works have the potential to revolutionize biosensing if one could find a way to manufacture hot particles reproducibly. Here we present results that provide a bridge between these two approaches. We demonstrate regular, electron-beam lithography (ebl) synthesized two-tier plasmonic nanostructures that show robust and reproducible large enhancements of far-field fluorescence measured using visible-light fluorescent agents.

Our nanostructures are comprised of two coaxial gold discs of different diameter stacked one on top of the other and separated by a dielectric spacer. Two different designs were explored, both being made by electron-beam lithography. The first design features a larger metallic disk of diameter D with a cylindrical hole of diameter d filled with a dielectric column produced by overexposed poly(methyl methacrylate) (PMMA) e-beam resist with a smaller metallic disk also of diameter d placed at the top of the column. A schematic and a scanning electron micrograph of a nanostructure of this design are shown in Figure 1a. We refer to this structure as a tower-type structure (TS). The fabrication of a structure of analogous geometry and their reflection spectra arising in the configuration of attenuated total reflectance have been discussed in ref 19. The second structure is topologically simpler, the large metallic disk with a hole is replaced by a solid disk; see Figure 1b. We refer to it as a pagoda-type structure (PS). Details of the fabrication of both structures are included in the Supporting Information. The smaller gold nanoparticle diameter d and the larger gold disk diameter D were varied in the submicrometer range.

To probe the field enhancement afforded by these structures, we coated them with a layer of a fluorescent dye, oxazine 1 perchlorate, randomly dispersed in a neutral polymer host, PMMA; see Figure 1a,b bottom panels. We excited the dye using a confocal laser arrangement with a laser (633 nm) and collected fluorescence in the 650−800 nm band. We showed experimentally in ref 20 that the

* To whom correspondence should be addressed. E-mail: sasha@manchester.ac.uk.
Received for review: 10/20/2009
Published on Web: 02/09/2010

DOI: 10.1021/nl903498h | *Nano Lett.* **2010,** *10,* 874–879

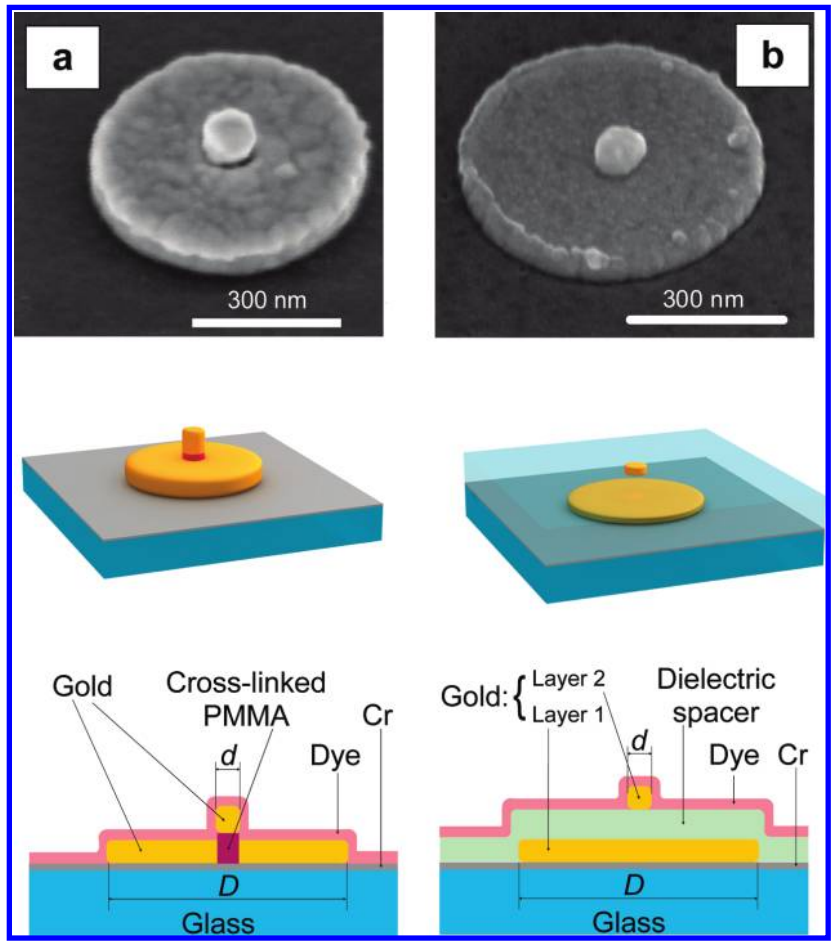

FIGURE 1. Schematic of composite nanostructures. (a) The tower-type structure. Top, SEM image; middle, schematic of TS; bottom, cross section of the structure with deposited dye. (b) The pagoda-type structure. Top, SEM image; middle, schematic of PS; bottom, cross-section of the structure with deposited dye.

fluorescence enhancement from simple gold nanostructures for this particular combination of dye and excitation wavelength is not affected by emission processes and can be attributed to the local enhancement of the electromagnetic field. (The possible effect of a change in the nonradiative decay rate for the composite nanostructures studied here is estimated in the Supporting Information where it is shown that any such effects should introduce an error of no more than ~20% in the calculated enhancements.) By comparing the fluorescence from the coaxial gold disk structures to that acquired from regions of the sample far from the metallic nanostructures, the field enhancement can be evaluated; see the detailed discussion in the Supporting Information.

Figure 2 demonstrates the main result of our report. For tower structures, fluorescence data from the small gold discs ($d \approx 100$ nm) on their own show a modest 1.5-fold far-field fluorescence enhancement above the background level (Figure 2a, left) in agreement with previous work.[20] The large gold discs $D \approx 600$ nm with the central hole $d \approx 100$ nm show some quenching of fluorescence near the center of the disk (Figure 2a, middle). This quenching is to be expected since the absence of a spacer layer over the metal means that much of the excitation from the dye layer is deactivated via the direct transfer of energy to the metal.[21,22] Remarkably, the two-tier tower structures show dramatic enhancement of the far-field peak fluorescence signal, 23-fold above the background (see Figure 2a right, which shows the far-field fluorescence signal normalized to the background level). Once normalized, the signal from the small disk on its own provides the peak value of the far-field fluorescence signal of about 0.5 above background. This implies that tower structures contribute to the far-field fluorescence signal (at its peak) about 46 times more than the small disk on its own. Supporting Information demonstrates that this factor (×46) represents a rough estimate for the ratio of the local fluorescence intensities above the small disk in the presence and in the absence of the second disk (cascade) of the tower structure. We refer to this enhancement factor as G_{CASC} (eqs 2, 9, and 13−15 of the Supporting Information). For pagoda structures the small discs also show a modest far-field fluorescence enhancement (Figure 2b, left) (slightly different from that obtained from the tower structures owing to the presence of a spacer layer between the chrome and the small disk). In contrast to the large disk of the tower

DOI: 10.1021/nl903498h | *Nano Lett.* **2010,** *10,* 874–879

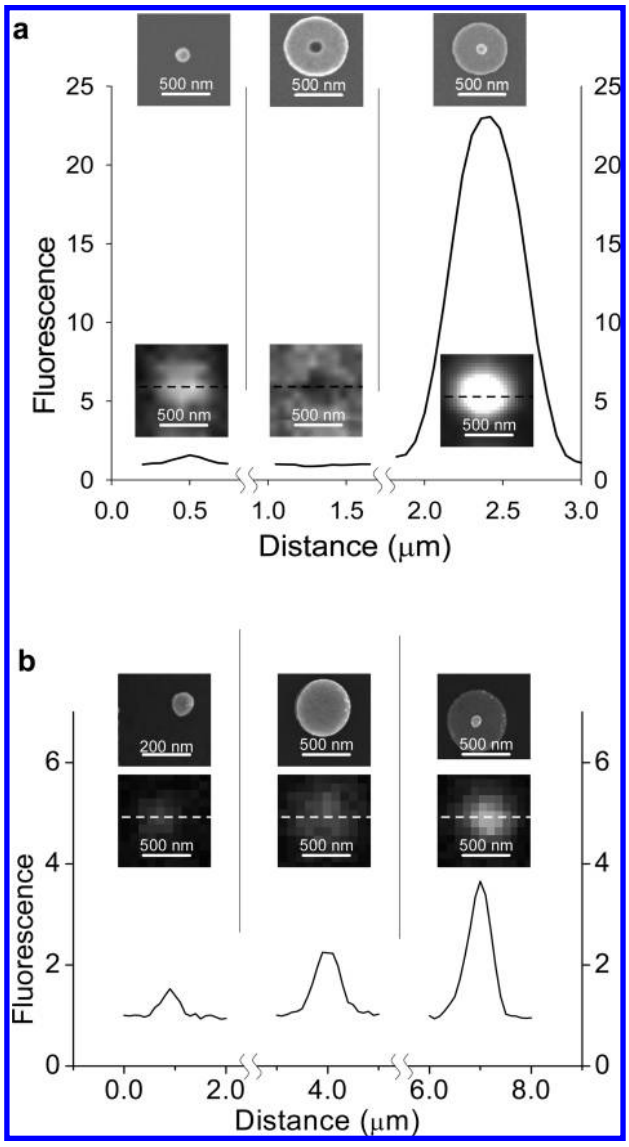

FIGURE 2. Far-field fluorescence signal from the nanostructures. (a) The tower-type structure. (b) The pagoda-type structure. The three panels show: left, far-field fluorescence signals from just the small disk on its own; middle, from the large disk on its own; and right, from the composite structure. The fluorescent signals are normalized to the background level. The sizes for TS are $d = 110$ nm, $D = 590$ nm, and for PS $d = 100$ nm, $D = 600$ nm. The top insets are scanning electron micrographs of the structures, the bottom insets show the fluorescence images, and dotted lines indicate line-scans for the graphs.

structures, the large disk of the pagoda structures shows a fluorescence enhancement since the 100 nm thick dielectric spacer-layer prevents quenching of the dye molecules (also, the dye is closer to the antinode of the standing wave produced by reflection from the large disk). Again, the two-tier pagoda structures show significantly enhanced peak values of the far-field fluorescence signal, 3.7 times larger than the background signal. This implies that pagoda structures contribute to the fluorescence signal (at its peak) about 5.4 times more than the small disk on its own. Although pagoda structures show smaller values of the fluorescence enhancement than tower structures, we include results from them here since pagoda structures have a simpler geometry and are easier to fabricate. Potentially, for thinner dielectric spacer layers, pagoda structures could yield a fluorescence enhancement comparable with tower structures, provided a fabrication problem (pinholes in the spacer layer) can be solved (see Supporting Information). It is worth noting that a two-tier structure for which the small disk is deposited directly on the top of the larger one (no spacer layer) showed no fluorescence enhancement over that obtained from the large disk on its own (data not shown).

To check the resonance properties of our structures we fabricated a set of tower structures where the sizes of both of the elements were varied. From the far-field fluorescence measured from these tower structures we extracted the coefficient of the enhancement ratio G_{CASC}. This coefficient measures the extent to which the field intensity above the small (top) disk is further enhanced by the presence of the larger (bottom) disk, see the detailed description in Supporting Information. As we will see below, we also made use of two other intensity enhancement factors, G_S and G_{NS}. The physical meaning of the intensity enhancements and enhancement ratios is as follows: G_S is a measure of the enhancement of the local field intensity near a single small disk; G_{CASC} indicates by how much this field above the small disk is further enhanced due to the presence of the large disk on its own; and G_{NS} gives the overall intensity enhancement above the small disk for the composite nanostructure. The three enhancement factors are related as follows: $G_{NS} = G_S G_{CASC}$. The procedures for the extraction of the enhancement ratios from measured far-field fluorescence data are given in the Supporting Information.

Figure 3a depicts G_{CASC} as a function of the size of the two particles (the ordinate is the size of smaller top particle while the coordinate shows the size of the bottom disk; the results are averages over data obtained from 50 nanostructures). Figure 3 reveals that there exist optimum values of d and D for the two cascades that yield the maximal value of G_{CASC}, $d \approx 110$ nm (Figure 3b) and $D \approx 590$ nm (Figure 3c). (Tower structures with these parameters also generated the largest far-field fluorescence signal.) The optimal size of the top particle of diameter of 110 nm corresponds to a disk that has its lowest order localized plasmon resonance mode at ~650 nm; see ref 20. Interestingly, the enhancement ratio G_{CASC} shows a much stronger dependence on the size of the bottom disk with the optimum size being close to the size of the first Fresnel zone $D_{Fr} \approx 590$ nm, as described in Supporting Information. This implies that the observed field enhancement might be influenced by both propagating-(intermediate) and near-fields although it could also be connected with the presence of the plasmonic modes of higher order in the larger bottom ring.[23] The dependency of G_{CASC} on the diameters of both discs shows that the composite structure needs to be tuned into resonance with the incident wave. It is worth noting that a lower disk of very

DOI: 10.1021/nl903498h | *Nano Lett.* **2010,** *10,* 874–879

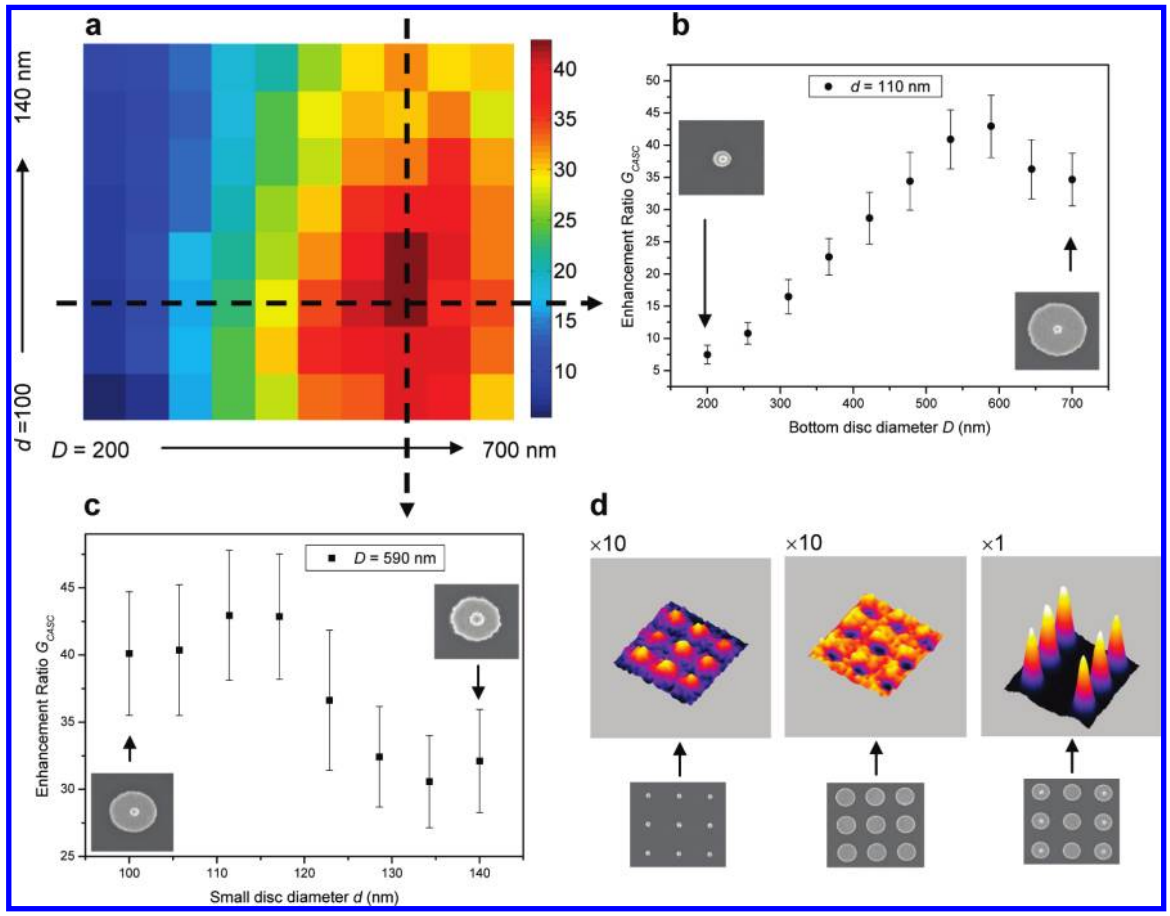

FIGURE 3. The enhancement of fluorescence. (a) The enhancement ratio of the field intensity, G_{CASC}, for TS as a function of the diameters of both the upper (smaller), d, and lower (larger) discs, D. (b) The dependence of G_{CASC} on D at the optimal value of $d = 110$ nm. (c) The dependence of G_{CASC} on d at the optimal value of $D = 590$ nm. (d) Three-dimensional plots of the fluorescence signal of an array of small discs (left), large discs (middle), and TS (right) with corresponding SEM micrographs below. Note that the signals from the small discs and large disk are multiplied by a factor of 10.

large size for tower structures, which approximates to an infinite plane layer of gold gave an enhancement ratio that was less than that of the peak enhancement by ~30% for the optimum size of the top nanoparticle $d \approx 110$ nm. Figure 3d provides a visual comparison of the fluorescence images obtained from small discs, large discs and tower structures. These data provide a very visual illustration of the enhancement afforded by the tower structures, especially when one notes the 10× magnification that has been applied to the data from the small and large discs (left and middle panels).

Now we turn to a quantitative description of the far-field fluorescence in our structures (see also Supporting Information). The Gaussian waist of the laser beam focused on a sample, w, was limited by the numerical aperture of the lens NA = 1.4 ($w > \lambda/(\pi \cdot \mathrm{NA}) \sim 140$ nm; this is the radius at which the field amplitude falls by 1/e). Because of the arrangement of the microscope optics, the actual value of w is larger and is quoted by the manufacturer to be $w \approx 200$ nm. To determine the degree of the field enhancement in an instrument-independent way we followed a procedure given elsewhere.[20] We integrated the measured fluorescence over a circular area centered on a structure (Supporting Information, Figure S2). The measurements were normalized against similar integrated measurements conducted over a background region, away from the presence of metallic nanostructures. These data (Supporting Information, Figure S2) have been used to determine the coefficient G_S showing the effective enhancement of the local field intensity in the vicinity of the small disk on its own, and the enhancement factor G_{CASC}. The parameter of particular interest here is the ratio of the effective intensity enhancement due to the nanostructure versus background, G_{NS}, which is the product of the enhancement due to the small disk and the extra boost this receives because of our two-tier cascade; $G_{NS} = G_S G_{CASC}$; see Figure S3. For tower structures, an enhancement factor, G_{NS}, of 900 ± 50 was calculated from the experimental data (Supporting Information, Figure S2) using a top-hat approximation of the spatial distribution of the field. This enhancement is a result of a 30-fold enhancement associated with the small disk only, G_S. A further factor of 30 arises because of the presence of the large disk, G_{CASC} (these data are derived from experiment). The field amplitude enhancement for the best two-tier structure was therefore $(G_{NS})^{1/2} \sim 30$ and was due to the 5−6 × field amplitude enhancement

DOI: 10.1021/nl903498h | *Nano Lett.* **2010,** *10,* 874–879

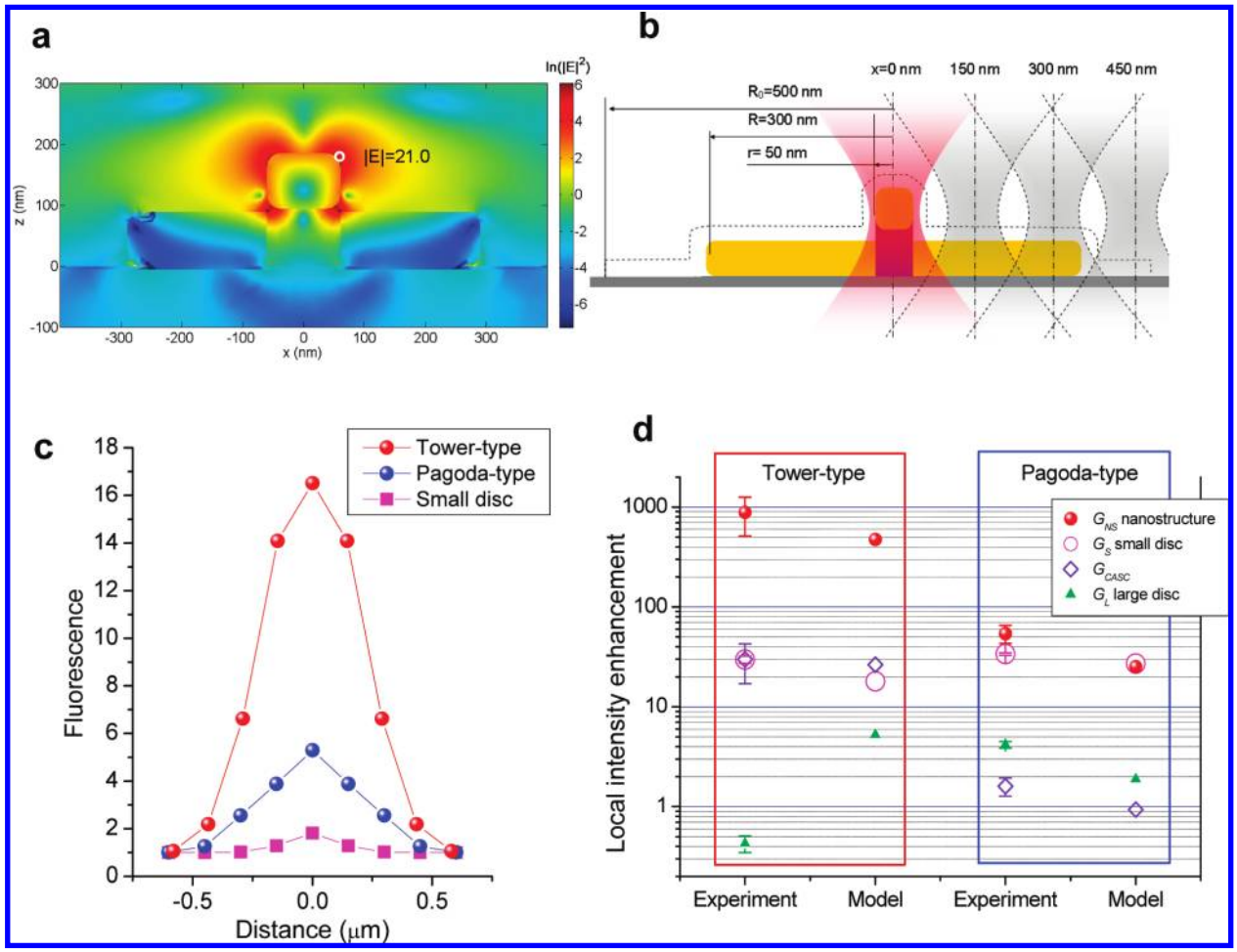

FIGURE 4. Finite element modeling of optical properties of nanostructures. (a) Calculated intensity of electromagnetic field near TS illuminated by a converging Gaussian beam ($w = 200$ nm). (b) Schematics of the calculations of the fluorescence signal observed in confocal microscope. (c) Fluorescent signal normalized over the background level calculated for TS with HFSS, compare with Figure 2. (d) Intensity enhancement ratio extracted from the measured fluorescence signals (Experiment) and calculated with HFSS (Model).

by a upper disk and another factor of 5−6 induced by the presence of the lower disk. These figures represent rough estimates obtained using the top-hat approximation; for further details see the Supporting Information. A higher level of field enhancement might be possible as we have calculated $G_{CASC} \approx 43 \pm 5$ from the peak values of the fluorescence signal (procedure B in Supporting Information), compared with $G_{CASC} \approx 30$ from integrating the fluorescence signal (procedure A in Supporting Information).

As a check on our measurements of the cascaded field enhancement, we performed finite-element modeling. We used a commercial package (HFSS ver. 11) to map the 3D field distribution produced by the structures in response to an incident field. Material constants at the required wavelength (633 nm) were measured using spectroscopic ellipsometry.[24] We assumed the incident beam had a Gaussian profile with the same width parameter as in the experiment. Figure 4a shows an example of the field profile over a vertical slice taken through a tower structure. These data show that the strongest fields are associated with the small particle, more specifically with the region between the smaller and larger particle for the combined two-tier structures. Using the 3D field maps, we obtained integrated fluorescence intensity data in a manner similar to those obtained from experiment (such data are also shown in Figure S2 and S3, Supporting Information). To mimic the scanning confocal experiment, the incident beam was centered on 5 points in the plane containing the upper disk, and the integrated fluorescence between these points was interpolated linearly; see Figure 4b,c. These calculated data were used to extract the far-field fluorescence signal and the total intensity enhancement of the structures (Figure 4d). The calculated data agree qualitatively with the experiments. A quantitative comparison of experimental data with the theory requires a thorough analysis of dye decay rates and hence dye quantum efficiency in the vicinity of studied nanostructures,[18,22,25−27] an analysis that goes beyond the scope of this report. The assumption of fixed quantum efficiency may lead to a change in the value of the field enhancement we calculate; however, in the Supporting Information we show that ignoring this aspect is unlikely to introduce an error of more than 20%.

DOI: 10.1021/nl903498h | *Nano Lett.* **2010,** *10,* 874–879

In summary, we have fabricated two-tier plasmonic nanostructures that exhibit reproducible and large electromagnetic field enhancements that can be successfully used for fluorescence studies in the visible part of the spectrum. We have further shown that the field enhancement is of resonant character. Finite-element modeling provides broad support for the experimental findings. The total local field enhancement for our best composite nanostructures was evaluated using a top-hat approximation as $(G_{NS})^{1/2} \sim 30$ times.

Acknowledgment. This work has been supported by EPSRC funding (EP/C534689/1 and EP/E01111X/1). W.L.B. is a Royal Society Wolfson Research Merit Award holder.

Supporting Information Available. Fabrication, characterization, analysis of the far-field fluorescence, finite element analysis of the nanostructures, accuracy of the effective intensity enhancement calculations, and Appendix. This material is available free of charge via the Internet at http://pubs.acs.org.

REFERENCES AND NOTES

(1) Kim, S.; et al. *Nature* **2008**, *453*, 757–760.
(2) Taminiau, T. H.; Stefani, F. D.; Segerink, F. B.; Van Hulst, N. F. *Nat. Photon.* **2008**, *2*, 234–237.
(3) Haes, A. J.; van Duyne, R. P. J. *J. Am. Chem. Soc.* **2002**, *124*, 10596–10604. Watanabe, K.; Menzel, D.; Nilius, N.; Freund, H.-J. *Chem. Rev.* **2006**, *106*, 4301–4320.
(4) Rothenhausler, B.; Knoll, W. *Nature* **1998**, *332*, 615–618.
(5) Michalet, X.; et al. *Science* **2005**, *307*, 538–544.
(6) Ledingham, K. W. D.; McKenna, P.; Singhal, R. P. *Science* **2003**, *300*, 1107–1111.
(7) Grier, D. G. *Nature* **2003**, *424*, 810–816.
(8) Hutter, E.; Fendler, J. H. *Adv. Mater.* **2002**, *16*, 1685–1706.
(9) Sarychev, V. K.; Shalaev, V. M. *Phys. Rep* **2000**, *335*, 275–371.
(10) Schuck, P. J.; et al. *Phys. Rev. Lett.* **2005**, *94*, No. 017402.
(11) Muhlschlegel, P.; et al. *Science* **2005**, *308*, 1607–1609.
(12) Li, K.; Stockman, M. I.; Bergman, D. J. *Phys. Rev. Lett.* **2003**, *91*, 227402.
(13) Righini, M.; Zelenia, A. S.; Girard, C.; Quidant, R. *Nat. Phys.* **2007**, *3*, 477–480.
(14) Grigorenko, A. N.; Roberts, N. W.; Dickinson, M. R.; Zhang, Y. *Nat. Photon.* **2008**, *2*, 365–370.
(15) Ghenuche, P.; et al. *Phys. Rev. Lett.* **2008**, *101*, 116805.
(16) Bardhan, R.; Grady, N. K.; Cole, J. R.; Joshi, A.; Halas, N. J. *ACS Nano* **2009**, *3*, 744–752.
(17) (a) Kneipp, K.; et al. *Phys. Rev. Lett.* **1997**, *78*, 1667–1670. (b) Nie, S.; Emory, S. R. *Science* **1997**, *275*, 1102–1106.
(18) (a) Anger, P.; Bharadwaj, P.; Novotny, L. *Phys. Rev. Lett.* **2006**, *96*, 113002. (b) Kuhn, S.; Hakanson, U.; Rogobete, L.; Sandoghdar, V. *Phys. Rev. Lett.* **2006**, *97*, No. 017402.
(19) Wang, S.; Pile, D. F. P.; Sun, C.; Zhang, X. *Nano Lett.* **2007**, *7*, 1076.
(20) Zoriniants, G.; Barnes, W. L. *New J. Phys.* **2008**, *10*, 105002.
(21) Pockrand, I.; Brillante, A.; Möbius, D. *Chem. Phys. Lett.* **1980**, *69*, 499–504.
(22) Barnes, W. L. *J. Mod. Opt.* **1998**, *45*, 661–669.
(23) Aizpurua, J.; et al. *Phys. Rev. Lett.* **2003**, *90*, No. 057401.
(24) Kravets, V. G.; Schedin, F.; Grigorenko, A. N. *Phys. Rev. B* **2008**, *78*, 205405.
(25) Dulkeith, E.; et al. *Phys. Rev. Lett.* **2002**, *89*, 203002.
(26) Dulkeith, E.; et al. *Nano Lett.* **2005**, *5*, 585.
(27) Anger, P.; Bharadwaj, P.; Novotny, L. *Phys. Rev. Lett.* **2006**, *96*, 113002.

DOI: 10.1021/nl903498h | *Nano Lett.* **2010,** *10,* 874–879